Strain-rate sensitivity of hardness of nanocrystalline $Ni_{75at.\%}Al_{25at.\%}$ alloy film

A.H.W. Ngan
Department of Mechanical Engineering, University of Hong Kong, Pokfulam Road, Hong Kong, People's Republic of China

J.B. Pethica
Department of Materials, University of Oxford, Parks Road, Oxford OX1 3PH, United Kingdom

H.P. Ng
Laboratoire des Matériaux et du Génie Physique, Ecole Nationale Supérieure de Physique de Grenoble-Institut National Polytechnique de Grenoble (ENSPG-INPG), UM 5628, BP 46, 38402, St. Martin d'Hères, France

(Received 1 September 2002; accepted 30 October 2002)

Room-temperature indentation experiments carried out on nanocrystalline $Ni_{75at.\%}Al_{25at.\%}$ alloy films with a range of grain sizes revealed that the strain-rate sensitivity of hardness is nearly zero and that the hardness increases as grain size decreases. The strain-rate insensitivity of hardness indicates that the room-temperature strength of these alloy films is dominated by an athermal, strain-rate-insensitive component. The hardness of the films was found to be in the range of 2.4 to 3.3 GPa, depending on grain size.

I. INTRODUCTION

When the grain size is reduced to the order of a few nanometers, it is often believed that dislocation activities will be suppressed.[1–4] The need to understand the deformation mechanisms of nanocrystalline materials under load therefore opens up a new direction of research. In particular, it has been found that when the grain size falls below a very small critical value, the Hall–Petch slope is nearly zero with little increase in strength on decreasing grain size, or even the inverse Hall–Petch behavior will occur, in which the strength actually decreases with decreasing grain size.[5]

Recent experiments on nanocrystalline copper also indicated the existence of a thermal and an athermal component of the flow strength.[6] The thermal component was found to have a strain-rate dependence of unity, i.e., strain rate is proportional to stress. This indicates a diffusive, Coble-creep-like mechanism.[7] When the deformation temperature is too low for diffusion to occur efficiently, the deformation mechanism is largely unknown. In this work, we performed room-temperature indentation experiments on a series of nanocrystalline $Ni_{75at.\%}Al_{25at.\%}$ alloy films to measure the strain-rate sensitivity and grain-size dependence of the strength (hardness) of this type of materials.

We selected depth-sensing indentation as a means of deforming the material because it is a technique in which the deformation condition can be well-controlled with minimal requirements on the sample geometry. Theoretical self-similarity and steady state of the deformation field can be achieved by using a load schedule in which the indentation load rate is proportional to the load P, i.e.,

$$\dot{P} = kP \quad \text{or} \quad P = P_o e^{kt} \quad , \tag{1}$$

where k is the desired constant strain rate, and P_o a small initial load.[8,9] We used a type of $Ni_{75at.\%}Al_{25at.\%}$ thin film sputter-deposited on nickel substrate as prototype nanocrystalline materials. The film thickness was about 3 μm, and the indentation depths were typically shallower than 0.5 μm, so in most cases the effect of the substrate was expected to be small. The grain size of the thin film in the as-deposited state was a few nanometers to roughly about 100 nm, depending on the heat-treatment conditions (Fig. 1). We used deposited thin films instead of bulk nanocrystalline specimens because the films prepared this way have a very smooth surface (roughness <10 nm on a 1 × 1 μm scan), which is important for nanoindentation experiments.

II. EXPERIMENTAL

The $Ni_{75at.\%}Al_{25at.\%}$ alloy thin films were prepared by direct current magnetron sputtering on nickel substrates using an alloyed target. As a continuous program in Hong Kong, the mechanical and electrical properties of this class of alloy thin films have been intensively investigated (see Refs. 10–16), and details regarding the film deposition can be found in these references. Worth

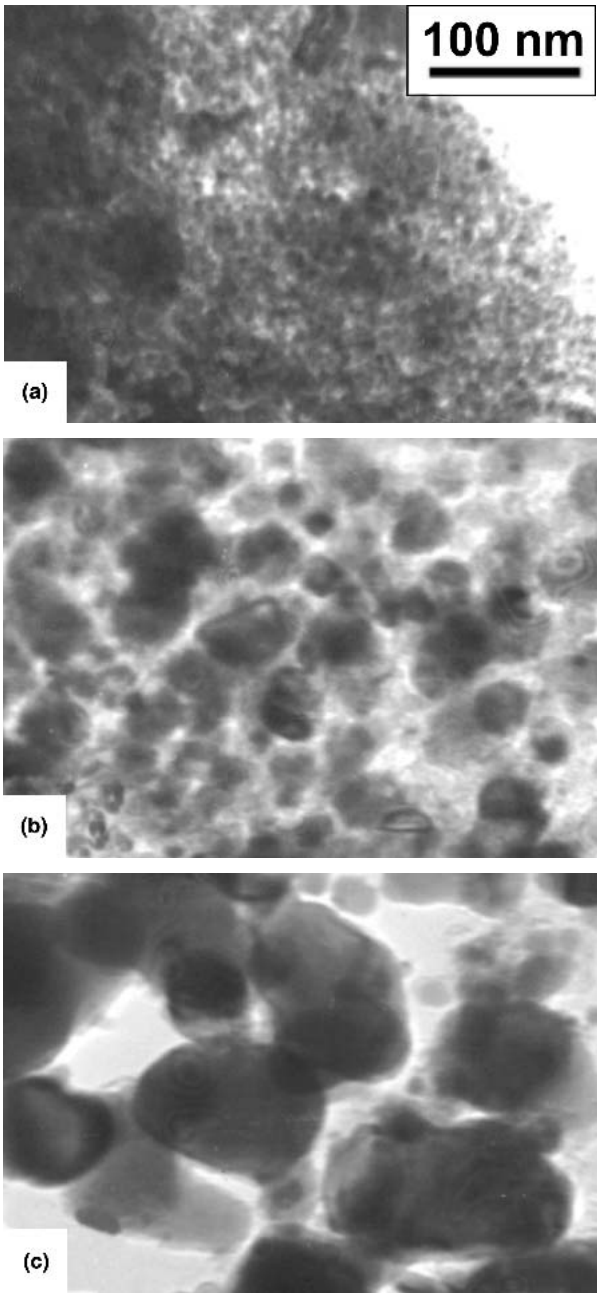

FIG. 1. Cross-sectional TEM bright-field micrographs of the $Ni_{75at.\%}Al_{25at.\%}$ alloy thin films used in this work: (a) As-deposited state, showing grain size of a few nanometers. (b) After post-deposition annealing at approximately 600 °C, showing grain size of about 40–50 nm. (c) After post-deposition annealing at approximately 800 °C, showing grain size of about 100 nm.

mentioning here is that the film in the as-deposited state without *in situ* substrate heating is nanocrystalline (Fig. 1) with a face-centered-cubic lattice structure.[12] Although the overall atomic ratio is 3Ni:1Al, there is a relatively large amount of oxygen incorporated into the film structure, as is typical in sputter-deposited films. Ordering into the equilibrium $L1_2$ phase happens only after heat treatment at, say, 700 °C. The grain size in these films can be controlled by suitable post-deposition heat treatment.[16] As shown in Fig. 1, the grain size in the as-deposited state is only a few nanometers. Upon heat treatment at approximately 600 °C, the grain size can be made to grow to about 40–50 nm, and at 800 °C, the grain size can become approximately 100 nm. In this work, we used an as-deposited film, a film heat treated at 400 °C, and one heat treated at 700 °C. The 400 °C film had grain size of about 10–20 nm, while the 700 °C film's grain size was about 50–100 nm. Further details about the grain growth kinetics of this type of $Ni_{75at.\%}Al_{25at.\%}$ thin films can be found in Ref. 16.

Indentation experiments were carried out at room temperature on a Nanoindenter II in Oxford (MTS Systems Corporation, MN) with a Berkovich tip. All results reported below were obtained using a load schedule consisting of a short preload segment to $P_o = 130$ μN under constant load rate for 10 s, followed by an exponential segment described by Eq. (1) to the same peak load of 40 mN, followed by unloading. It should be noted that the exponential load schedule in Eq. (1) would give rise to a constant strain rate k only during steady state, i.e., when the observed hardness is constant. For this reason, initial transient responses were ignored in the analyses below. The machine had the fastest loading rate corresponding to a strain rate k [Eq. (1)] of about 0.28 s^{-1}, and this corresponds to an overall test duration of about 30 s. The slowest strain rate used was $k = 1 \times 10^{-4}$ s^{-1}, corresponding to a test duration of about 16 h. For the slow experiments, the effect of thermal drift on the recorded displacement data was tremendous. Taking a typical drift rate of 0.01 nm s^{-1} as an example, the amount of drift during 16 h would be about 576 nm, and this is even larger than the displacement of about 500 nm at peak load recorded in a fast indentation experiment. In view of this, all experiments were carried out using the continuous stiffness mode, in which the contact stiffness S was recorded at regular intervals under a small alternating current (ac) force modulation at approximately 40 Hz. S measured this way is free from influence by thermal drift, and hence no drift correction is required. From contact mechanics, the contact radius a between the tip and the specimen surface is proportional to S, namely,

$$S = 2\,E_r a = 2\,E_r h \tan\psi \quad , \tag{2}$$

where E_r is the reduced modulus, h is the indenter displacement, and ψ is the semi-angle of the indenter. S is therefore a direct measure of the contact size.[17–19] The hardness $P/\pi a^2$ of the specimen is therefore measured by the quantity P/S^2.

A series of control experiments using similar indentation conditions was conducted on a polycrystalline indium sample with a grain size of a few millimeters. The

indium specimen was annealed and its top surface electropolished. Details of the preparation procedures can be found in Ref. 20.

III. RESULTS

Figure 2 shows the effect of strain rate on the hardness characterized by P/S^2 in the as-deposited $Ni_{75at.\%}Al_{25at.\%}$ nanocrystalline thin film. It can be seen that the hardness settles down to a steady-state value at each strain rate as load or time increases. It is also evident that the steady-state hardness shows no clear change at all over a strain-rate change of 2800 times from 1×10^{-4} s^{-1} to 0.28 s^{-1}. The strain-rate sensitivity of hardness in this case is therefore very close to zero. Figures 3 and 4 show, respectively, the P/S^2 versus load plots of the 400 and 700 °C annealed films. It can be seen that the hardness also became quite steady at large loads, although it seems that the steadiness is not as good as that in the as-deposited film. The hardness data at different strain rates for the annealed films also seem to scatter a little more compared with the as-deposited film, but repeated testing using the same experimental conditions showed that the scatter is purely random, and there is no clear trend of hardness increasing or decreasing as strain rate increases. In other words, one must conclude that the strain-rate sensitivity of hardness for the annealed films is also very close to zero.

To show that a strong strain-rate dependence of hardness can indeed be detected by this indentation technique, control experiments on indium were performed. Indium has a melting point of 157 °C and room temperature corresponds to 0.7 T_m. Deformation is therefore likely to be diffusion controlled (e.g., dislocation creep), and the hardness of indium is known to exhibit a strong dependence on strain rate.[8] As shown in Fig. 5, an obvious trend of decreasing P/S^2 as k decreases is indeed observed in our indium sample with our machine. The stress exponent estimated from these data is about 3.2.

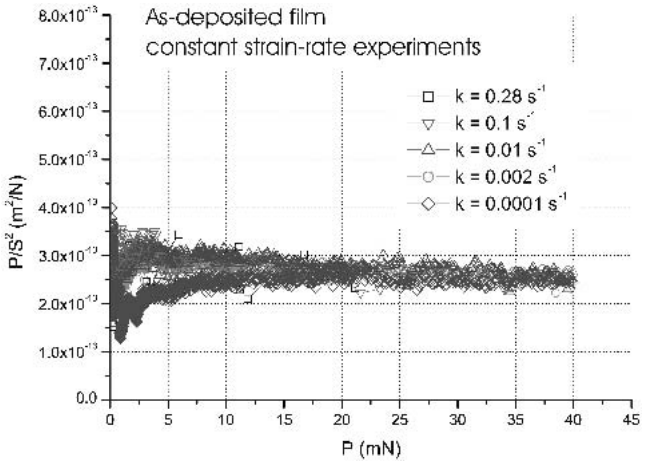

FIG. 2. Hardness versus load in as-deposited nanocrystalline $Ni_{75at.\%}Al_{25at.\%}$ thin film.

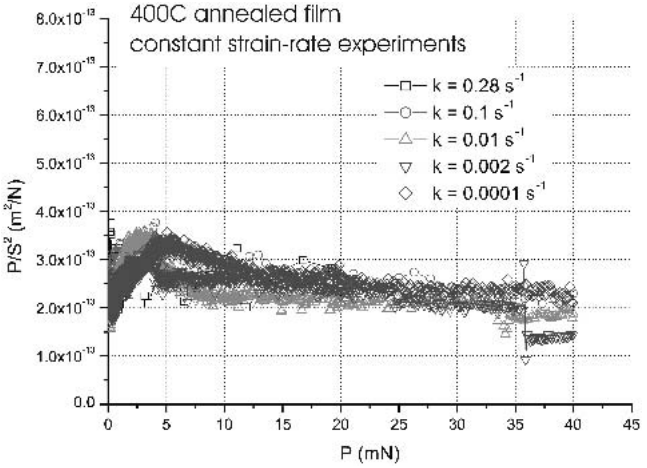

FIG. 3. Hardness versus load in 400 °C annealed nanocrystalline $Ni_{75at.\%}Al_{25at.\%}$ thin film.

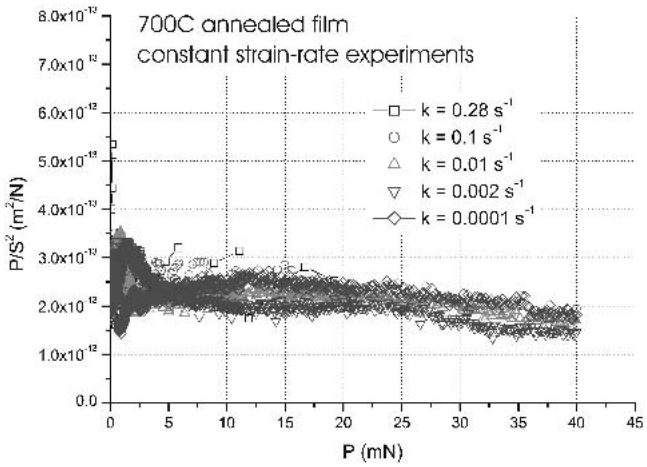

FIG. 4. Hardness versus load in 700 °C annealed nanocrystalline $Ni_{75at.\%}Al_{25at.\%}$ thin film.

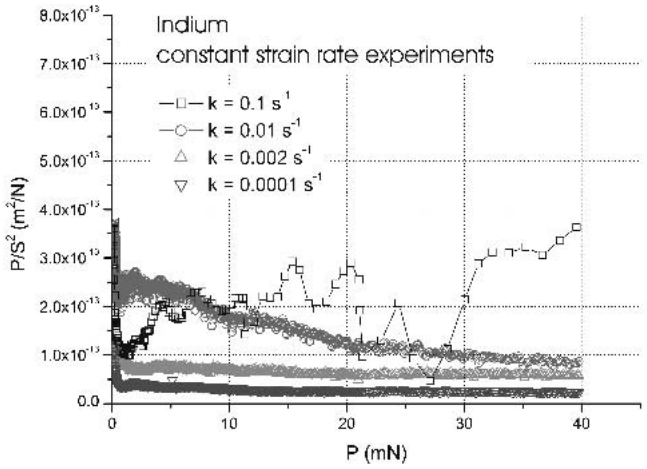

FIG. 5. Hardness versus load in bulk indium.

Diffusional creep mechanisms (Herring–Nabarro or Coble) are Newtonian-like and have even stronger strain-rate dependence than this. Hence, if diffusional creep mechanisms were active in our nanocrystalline films, the observed strain-rate dependence of hardness would have been prominent.

A quantitative measure of the hardness of our nanocrystalline films can be obtained by calibrating the contact stiffness (S) data against the displacement (h) data. As mentioned beforehand, the displacement data should be accurate when the test duration is small, as any drifts would have minute effects. This can be illustrated by Fig. 6, which shows the S-h plots from independent indentation experiments on the as-deposited film. It can be seen that for the fast experiments ($k = 0.28$ or $0.1\ s^{-1}$), the plots are nearly identical, but for the slow experiments ($k \leqslant 1 \times 10^{-2}\ s^{-1}$), the h data have been severely affected by drifts so that plots from different runs can no longer be overlaid on top of one another. Moreover, in the fast experiments, S is observed to be proportional to h during loading as shown in Fig. 6, thus Eq. (2) is verified. The slope S/h of the loading portion of the high strain rate data in Fig. 6 is approximately 5.7×10^{11} Pa, and the E_r worked out from $S/h = 2E_r \tan \psi$ [Eq. (2)], is about 97 GPa. From Fig. 2, the steady value of P/S^2 is about 2.5×10^{-13} m^2/N, and hence the hardness of the as-deposited film is

$$H = \frac{P}{24.5h^2} = \frac{P}{24.5S^2}\left(\frac{S}{h}\right)^2 = \frac{2.5 \times 10^{-13}}{24.5} \times (5.7 \times 10^{11})^2 = 3.3\ \text{GPa} \quad . \tag{3}$$

Assuming the macroscopic tensile yield strength to be one-third of the hardness,[21] the yield strength of the as-deposited film is about 1.1 GPa. Using a continuum analysis from an independent set of microhardness experiments on similar $Ni_{75at.\%}Al_{25at.\%}$ nanocrystalline films,[14,15] the yield strength of this type of film in the as-deposited state was estimated to be about 1.4 GPa. The two estimates of strength are therefore in agreement.

Similar analyses were applied to the 400 and 700 °C annealed films. As can be seen by comparing Figs. 2 and 4, the steady state P/S^2 value of the as-deposited film appears to be higher than that of the 400 °C annealed film, which in turn is higher than that of the 700 °C annealed film. The slope S/h of the loading portion of the high-strain-rate data from the annealed films was found to be roughly the same as that of the as-deposited film, as shown in Fig. 6. This indicates that, as can be seen from Eq. (2), the elastic modulus of the film is not critically affected by annealing or grain growth. Using the observed steady-state P/S^2 values from Eq. (3), the hardness of the 400 and 700 °C annealed films was determined to be about 2.6 and 2.4 GPa, respectively. In other words, the hardness of our $Ni_{75at.\%}Al_{25at.\%}$ thin films decreases from about 3.3 to 2.4 GPa upon heat treatment and the associated grain growth from a few nanometers to 50–100 nm.

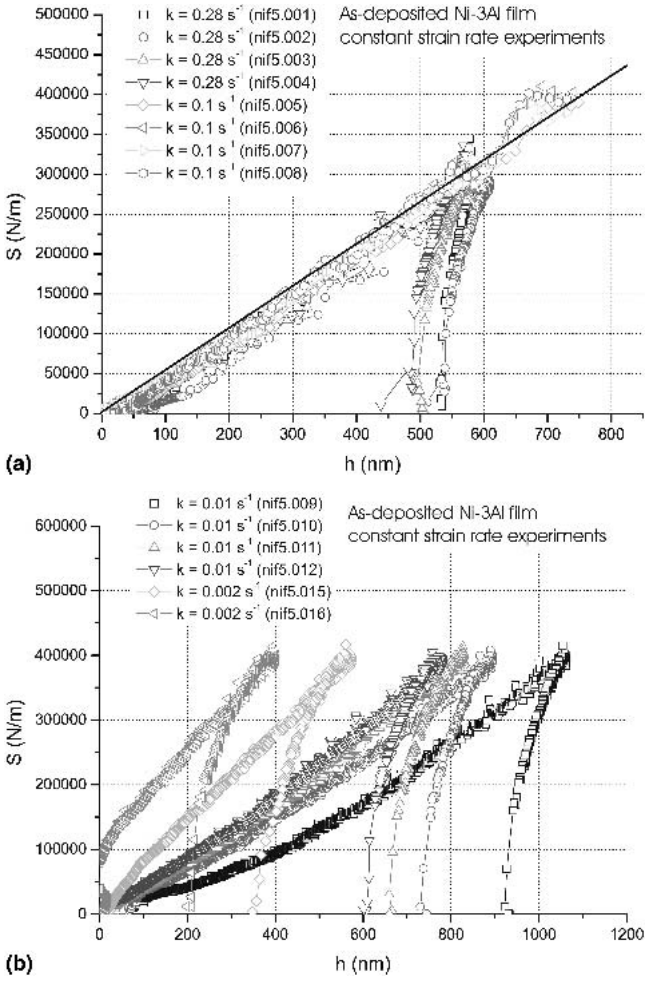

FIG. 6. Contact stiffness (S) versus displacement (h) plots during loading and unloading in as-deposited nanocrystalline $Ni_{75at.\%}Al_{25at.\%}$ thin film.

IV. DISCUSSION

The above results show that the strain-rate sensitivity of the hardness in our nanocrystalline films is nearly zero. This contradicts the existence of an important diffusive component at room temperature in this material. In other words, the room-temperature strength of this material is dominated by an athermal, strain-rate-insensitive component. This is interesting contrast to earlier tensile test results on nanocrystalline copper by Cai *et al.*,[6] who have shown the existence of both a thermal and athermal component describable by the flow law

$$\dot{\epsilon} = C\ (\sigma - \sigma_o) \quad , \tag{4}$$

where $\dot{\epsilon}$ is the strain rate, σ the applied stress, σ_o a constant threshold stress (the athermal component), and C a constant containing the Boltzmann factor. The

experimental conditions in the two investigations are, however, very different. The strain-rate range in the current experiments is a change by 2800 times from 1×10^{-4} s^{-1} to 0.28 s^{-1}, and this is a much larger range than the rate range used by Cai *et al.*, which was from 2×10^{-7} s^{-1} to 17×10^{-7} s^{-1}, i.e., a change of only 8.5 times. In other words, the flow rule in Eq. (4) was really concluded from a very narrow $\dot{\epsilon}$ range, and its applicability to the wider domain is uncertain. Moreover, the strain rates used in the current experiments are at least three orders of magnitude higher than those used by Cai *et al.*, and so the deformation conditions may not be comparable. In any case, the athermal stress σ_o found by these authors was about 130 ± 10 MPa, and this is much larger than the change in stress of ≤20 MPa observed in the strain-rate range they used. In other words, even though the thermal component exists in Cai *et al.*'s situation, the dominating component seems to be the athermal component.

We also found that the hardness of our thin films is a decreasing function of grain size. This is in agreement with many previous investigations using bulk nanocrystalline specimens.[5] If the mean grain sizes were 3, 15, and 75 nm for the as-deposited, 400 °C annealed and 700 °C annealed films, respectively, the corresponding measured hardness data of 3.3, 2.6, and 2.4 GPa would fall accurately onto a Hall–Petch plot with the grain-size exponent being –0.5. However, a wider range of grain size would be required to unambiguously verify the Hall–Petch relation or to disprove other functional dependence involving, for example, a different grain-size exponent.

V. CONCLUSIONS

Room-temperature indentation experiments were performed on a series of nanocrystalline $Ni_{75at.\%}Al_{25at.\%}$ alloy films to measure the strain-rate sensitivity of hardness of this material. The strain-rate sensitivity of hardness was found to be zero. This indicates that the room-temperature strength of this material is dominated by an athermal, strain-rate insensitive component. The measured hardness in our nanocrystalline $Ni_{75at.\%}Al_{25at.\%}$ alloy films was found to decrease from about 3.3 GPa to 2.4 GPa when the grain size increased from a few nanometers to roughly 50–100 nm.

ACKNOWLEDGMENTS

We thank Dr. Musuvathi S. Bobji for his assistance on the Nanoindenter II in Oxford. A major part of the work was completed during A.H.W.N.'s sabbatical leave at Oxford. Financial support in the form of a travel grant from the University of Hong Kong and provision of laboratory facilities by the host department are gratefully acknowledged. The project was supported by two research grants from the Research Grants Council of the Hong Kong Special Administrative Region, China (Project Nos. HKU 7062/01E and HKU 7083/02E).

REFERENCES

1. P. Gao and H. Gleiter, Acta Metall. **35,** 1571 (1987).
2. G.J. Thomas, R.W. Siegel, and J.A. Eastman, Scripta Metall. Mater. **24,** 201 (1990).
3. W.W. Milligan, S.A. Hackney, M. Ke, and E.C. Aifantis, Nanostruct. Mater. **2,** 267 (1993).
4. J. Schiotz, F.D. Di Tolla, and K.W. Jacobsen, Nature **391,** 561 (1998).
5. M.Yu. Gutkin, I.A. Ovid'ko, and C.S. Pande, Rev. Adv. Mater. Sci. **2,** 80 (2001).
6. B. Cai, Q.P. Kong, L. Lu, and K. Lu, Scripta Mater. **41,** 755 (1999).
7. M.F. Ashby and R.A. Verrall, Acta Metall. **21,** 149 (1973).
8. B.N. Lucas and W.C. Oliver, Metall. Mater. Trans. **30A,** 601 (1999).
9. A.F. Bower, N.A. Fleck, A. Needleman, and N. Ogbonna, Proc. R. Soc. (London) A **441,** 97 (1993).
10. H.P. Ng, X.K. Meng, and A.H.W. Ngan, Scripta Mater. **39,** 1737 (1998).
11. H.P. Ng, PhD Thesis, University of Hong Kong, Hong Kong, People's Republic of China (2000).
12. H.P. Ng and A.H.W. Ngan, J. Appl. Phys. **88,** 2609 (2000).
13. H.P. Ng and A.H.W. Ngan, in *Nanophase and Nanocomposite Materials III,* edited by S. Komarneni, J.C. Parker, and H. Hahn (Mater. Res. Soc. Symp. Proc. **581,** Warrendale, PA, 2000), p. 571.
14. S.Y. Li, H.P. Ng, and A.H.W. Ngan, in *Fundamentals of Nanoindentation and Nanotribiology II,* edited by S.P. Baker, R.F. Cook, S.G. Corcoran, and N.R. Moody (Mater. Res. Soc. Symp. Proc. **649,** Warrendale, PA, 2001).
15. A.H.W. Ngan and H.P. Ng, in *Advances in Fracture Research,* Electronic proceedings of 10th International Congress on Fracture (on CD ROM), edited by K. Ravi-Chandar, B.L. Karihaloo, T. Kishi, R.O. Ritchie, A.T. Yokobori Jr., and T. Yokobori (Pergamon), paper no. 0540.
16. H.P. Ng and A.H.W. Ngan, J. Mater. Res. **17,** 2085 (2002).
17. J.B. Pethica and W.C. Oliver, in *Thin Films: Stresses and Mechanical Properties,* edited by J.C. Bravman, W.D. Nix, D.M. Barnett, and D.A. Smith (Mater. Res. Soc. Symp. Proc. **130,** Pittsburgh, PA, 1989), p. 13.
18. T.P. Weighs and J.B. Pethica, in *Shape-Memory Materials and Phenomena—Fundamental Aspects and Applications,* edited by C.T. Liu, M. Wuttig, K. Otsuka, and H. Kunsmann (Mater. Res. Soc. Symp. Proc. **246,** Pittsburgh, PA, 1992), p. 325.
19. S.A. Syed Asif and J.B. Pethica, Philos. Mag. A **76,** 1105 (1997).
20. G. Feng and A.H.W. Ngan, Scripta Mater. **45,** 971 (2001).
21. D. Tabor, *The Hardness of Metals* (Oxford University Press, Oxford, U.K., 1951).